



## OPEN Bathymetry and environmental features govern the microbial communities in mesopelagic sediments of the Lakshadweep Islands of India

T. G. Sumithra<sup>1</sup>, S. Gayathri<sup>1</sup>, Vijayakumar S. Mannur<sup>1</sup>, N. Neethu<sup>1</sup>, R. Ratheesh Kumar<sup>1</sup>, Anusree V. Nair<sup>1</sup>, Lavanya Ratheesh<sup>1</sup>, P. M. Zainul Abid<sup>1</sup>, B. Karpaga Raja Sundari<sup>2</sup>, G. Dharani<sup>2</sup> & S. R. Krupesh Sharma<sup>1</sup>✉

Mesopelagic sediments represent a critical yet understudied component of marine ecosystems, where environmental gradients strongly influence microbial community structure and function. This study profiles prokaryotic and fungal communities in the sediments along a bathymetric transect (500–1000 m) on the upper continental slope of the Lakshadweep Sea to identify community assembly processes and environmental drivers. Mesopelagic sediments supported diverse prokaryotic and fungal assemblages, with prokaryotes exhibiting higher  $\alpha$ -diversity indices than fungi, indicating differential ecological adaptation of prokaryotic and fungal groups. *Bacteria* dominated over *Archaea*, with Firmicutes, Chloroflexi, Bacteroidota, Proteobacteria, and Desulfobacterota as the major prokaryotic phyla. Ascomycota and Basidiomycota were the major fungi. Diversity varied significantly ( $p \leq 0.05$ ) with depth, and most microbes were habitat specialists, indicating strong vertical structuring. The FEAST analysis revealed a limited proportional contribution of microbial communities in deeper sediments from 500 m. Beta nearest taxon index analysis suggested a dominant role of deterministic processes in governing the microbial community assembly. Canonical correspondence analysis identified temperature and DO as key drivers of prokaryotes, and nitrogen and temperature for fungi. Depth was significantly correlated ( $p \leq 0.05$ ) with the relative abundance of certain microbial taxa, including a decline in bacterial abundance and an increase in archaeal abundance, as well as positive associations with Dadabacteria, Halobacterota, and Chytridiomycota. This first study from the Lakshadweep Sea provides new insights into tropical mesopelagic sediment microbial diversity and community assembly, highlighting bathymetric and environmental controls that shape the prokaryotic and fungal communities.

**Keywords** Prokaryotic diversity, Fungal diversity, Deep Sea, Microbial community assembly

The deep seafloor (> 200 m) covers nearly 67% of Earth's lithosphere, making it the largest ecological realm on the planet<sup>1</sup>. Despite the prevailing extreme conditions, such as perpetual darkness, low organic nutrient availability, high pressures, and low temperatures, the deep seafloor harbours a remarkably rich, yet untapped, microbial biodiversity that drives nutrient recycling, carbon sequestration, and global biogeochemical cycles, thereby influencing ecosystem functioning at both regional and global scales<sup>2</sup>. Growing anthropogenic pressures, including climate change, marine littering, and industrial exploitation of deep-sea resources, have raised serious concerns about the sustainability of deep-sea biodiversity and highlighted the lack of effective conservation strategies for seabed habitats<sup>3</sup>. Understanding how microbial assemblages vary across bathymetric and environmental gradients is therefore critical for predicting ecosystem responses to natural and anthropogenic changes. However, deep-sea research remains constrained by the high costs and logistical challenges of benthic sampling, resulting in a sparse knowledge base relative to the vastness of the habitat. Among the various deep-sea

<sup>1</sup>ICAR-Central Marine Fisheries Research Institute (CMFRI), Post Box No. 1603, Ernakulam North P.O., Kochi 682018, India. <sup>2</sup>National Institute of Ocean Technology, Ministry of Earth Sciences, Chennai 600100, India. ✉email: krupeshsharma@gmail.com; krupesh.sharma@icar.org.in

zones, the mesopelagic zone (200 to 1000 m) plays a crucial role in regulating the global climate and supporting deep-sea ecosystems. Although knowledge of mesopelagic microbial communities is very limited, increasing evidence suggests that the mesopelagic zone is a unique reservoir of microbial diversity<sup>4</sup>. Furthermore, Baltar et al.<sup>5</sup> noted that regional differences in microbial functioning are more pronounced within the mesopelagic realm than within the epipelagic realm. These findings were unexpected, since the epipelagic zone usually shows greater regional variation, whereas the deep ocean is considered more uniform, with stable microbial communities and low activity, raising more curiosity about the microbial communities of the mesopelagic zone. In this study, we investigated microbial communities in sediments collected from the upper continental slope within the mesopelagic depth range.

Recent studies have revealed that prokaryotes (Bacteria and Archaea) dominate deep-sea sediments, contributing ~ 90% of benthic biomass<sup>6</sup>. In contrast, the diversity of fungi in deep-sea sediments remains less explored, though certain studies revealed unexpectedly rich fungal communities in different deep-sea habitats<sup>7,8</sup>. Moreover, bathymetric gradients, along with associated shifts in various environmental drivers, exert a strong influence on microbial community structure in marine sediments<sup>9</sup>. While depth-related variations in bacterial and fungal communities have been reported from different oceanic regions<sup>10,11</sup>, comprehensive information on these patterns in tropical deep-sea ecosystems, particularly in the Indian Ocean, remains limited, representing a critical knowledge gap. Furthermore, while depth-related microbial community variations in the mesopelagic zone have been documented<sup>12</sup>, studies focusing on the sedimentary environments of the tropical Indian Ocean remain limited.

The Lakshadweep Sea, situated in the northeastern Arabian Sea, is an ecologically and biogeographically distinct region of the Indian Ocean<sup>13</sup>. The Lakshadweep Sea is characterised by wide-ranging coral reef ecosystems of the Lakshadweep archipelago, and unique oceanographic processes, including monsoon-driven circulation and seasonal upwelling, which influence nutrient dynamics and productivity. As a transition zone between coastal and open-ocean systems, characterised by steep bathymetric gradients and reef-associated habitats, it supports diverse pelagic and benthic communities and exhibits high microbial niche heterogeneity<sup>13</sup>. However, information on benthic microbial diversity and depth-related patterns in this region remains scarce. Previous work by Kumbhare et al.<sup>14</sup> examined bacterial communities in shallow sediments (< 50 m) off Agatti Island, Lakshadweep Sea, but deeper zones remain unexplored. Here, we employed high-throughput sequencing of the 16 S rRNA gene and ITS region to explore the bacterial, archaeal, and fungal communities in the sediments along a bathymetric transect (500, 750, and 1000 m) on the upper continental slope of the Lakshadweep Sea. We also aimed to characterise whether mesopelagic sediment microbial communities exhibit depth-dependent variations and, if so, what are the key environmental drivers shaping these assemblages. We employed community assembly analyses ( $\beta$ -nearest taxon index) to disentangle deterministic and stochastic processes, and used multivariate analysis (canonical correspondence analysis) to identify key environmental drivers influencing community distribution. Our findings contribute to a broader understanding of microbial biogeography in the Indian Ocean and provide a foundation for future studies on the functioning of tropical deep-sea ecosystems.

## Materials and methods

### Sample collection

Deep-sea sediment samples from the Lakshadweep Sea were collected during a research cruise through the FV Silver Pompano (FVSP/2025/5) in the Lakshadweep Sea during February 2025 along the upper continental slope at depths of 500 m, 750 m, and 1000 m (Fig. 1). In detail, station 1 (10°07.993' N, 075°37.190' E), station 2 (10°19.000' N, 075°34.004' E), and station 3 (10°05.071' N, 075°29.774' E) corresponded to sampling depths of 500 m, 750 m, and 1000 m, respectively. At each depth, triplicate ( $n = 3$ ) samples were obtained using a Van Veen grab sampler (surface area: 1000 cm<sup>2</sup>; ~ 60 kg). Accordingly, there were 9 samples representing three depths with triplicate sediment replicates from each depth. The top ~ 5 cm of undisturbed sediment was subsampled aseptically into sterile containers. The samples were immediately frozen at -20 °C until processing in the laboratory at ICAR-CMFRI. Parallel subsamples were preserved at 4 °C for sediment geochemical analyses.

As the study involved only sediment samples and did not include live animals, plants, or human subjects, formal ethical approval was not required.

### Environmental parameters

In situ hydrographic parameters were measured using a CTD (Conductivity Temperature Depth) profiler (Model: 19Plus; Sea-Bird Scientific SBE 19plus V2 SEACAT, Washington) equipped with auxiliary sensors. The measurement accuracies for the CTD sensors were as follows: conductivity,  $\pm 0.0005$  S/m; temperature,  $\pm 0.005$  °C; and pressure,  $\pm 0.1\%$  of full-scale range (strain gauge). Additional sensors were used to monitor dissolved oxygen (DO), turbidity, pH, chlorophyll fluorescence, oxygen saturation, and photosynthetically active radiation (PAR). DO was measured using an SBE 43 polarographic membrane sensor with an accuracy of  $\pm 2\%$  of saturation. Bio-optical properties were obtained using a WET Labs ECO FLNTU sensor, which measured chlorophyll-a fluorescence (470/695 nm; sensitivity 0.025  $\mu\text{g L}^{-1}$ ) and turbidity (700 nm; sensitivity 0.01 NTU). PAR (400–700 nm) was measured using a cosine-corrected sensor with a range of 0–5000  $\mu\text{mol photons m}^{-2} \text{s}^{-1}$ . The system was further equipped with an altimeter for precise bottom tracking and supported additional inputs for pH measurement. Oxygen saturation was calculated from dissolved oxygen and temperature data. All sensors were calibrated before deployment, in accordance with the manufacturer's guidelines. Data were processed using the Sea-Bird Seasoft V2 software, including application of factory calibration coefficients, temporal alignment of sensors, and bin-averaging at 1 m intervals. In addition, elemental composition (C, H, N, and S) of sediments was quantified using a CHNS elemental analyser (Model: Unicube; Elementar, Germany) following the manufacturer's protocol. Analysis of proteins in deep-sea sediments was carried out spectrophotometrically

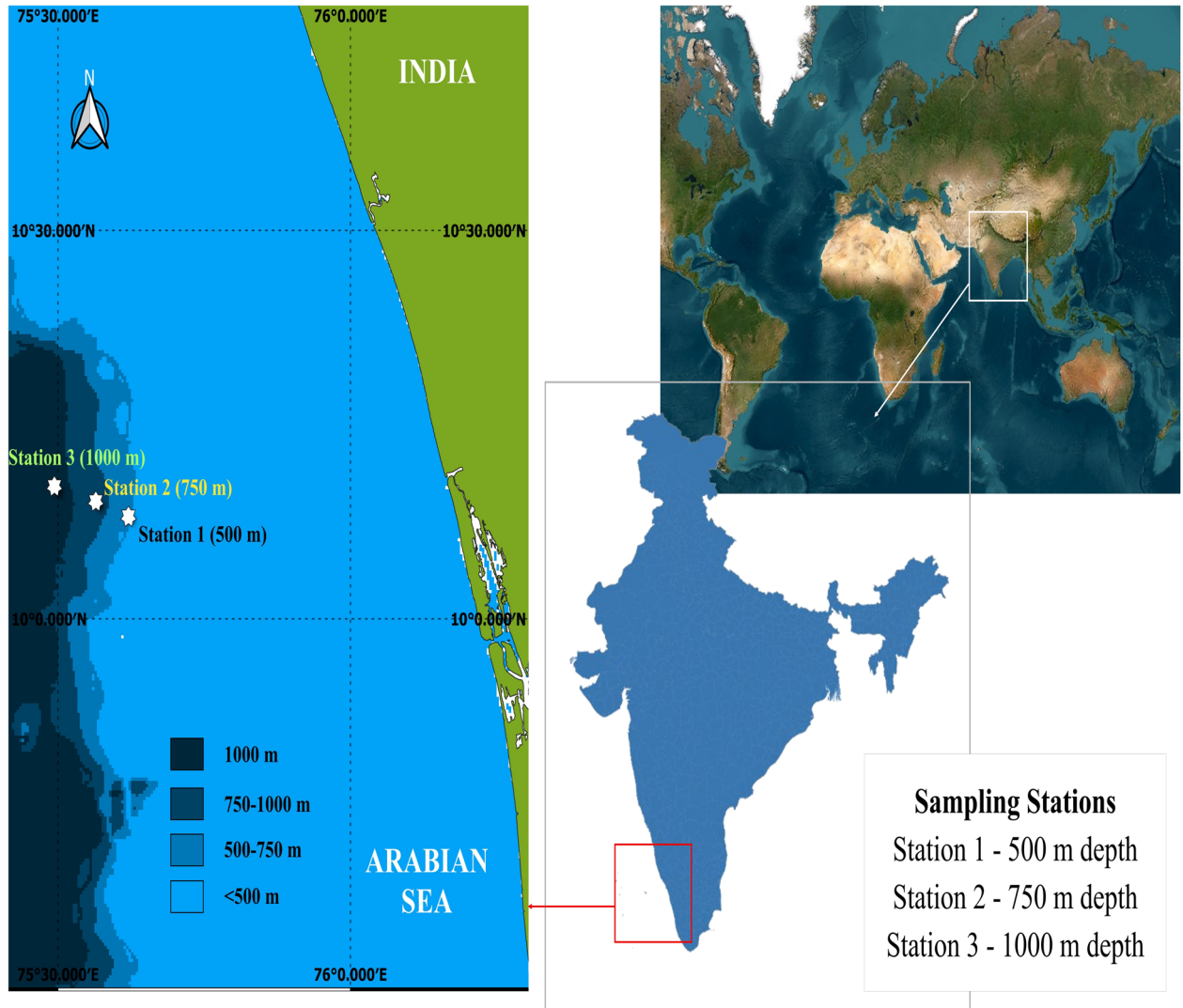


**Fig. 1.** Sampling stations of the present study. \*Denotes the different sampling stations. Station 1 ( $10^{\circ}07.993'$  N,  $075^{\circ}37.190'$  E), Station 2 ( $10^{\circ}19.000'$  N,  $075^{\circ}34.004'$  E), and Station 3 ( $10^{\circ}05.071'$  N,  $075^{\circ}29.774'$  E) correspond to sampling depths of 500 m, 750 m, and 1000 m, respectively. The map in this figure was generated using QGIS desktop app version 3.40.6. The URL link to access or download the software app is <https://qgis.org/download/>. GEBCO (General Bathymetric Chart of the Ocean) <https://www.gebco.net/> was used to download the recent bathymetric map of Arabian sea, India. The ocean bed at varying levels such as < 500 m, 500 to 750 m, 750 to 1000 m and > 1000 m was distinguished using QGIS. The station points were specified by adding a csv (Comma-separated values) excel file containing latitude and longitude information in the Action QGIS Window.

using Lowry's method<sup>15</sup>. The standard curve was generated using a known concentration of bovine serum albumin as a protein standard.

#### DNA extraction, amplification, library preparation and sequencing

DNA extraction was performed from ~ 0.5 g of sediment using the DNeasy PowerSoil Pro Kit (Cat. No. 47104, Qiagen) according to the manufacturer's protocol. The concentration and purity of the extracted DNA were assessed using a NanoDrop 2000 spectrophotometer (Thermo Fisher Scientific, MA, USA). DNA integrity was further confirmed by electrophoresis on a 1% agarose gel (Lonza, Belgium). We performed additional extractions on the samples that yielded low amounts of DNA, and the DNA derived from these samples was then combined and concentrated. The extracted DNA samples were deemed suitable for PCR amplification. For prokaryotic community profiling, the V3-V4 region of the 16 S rRNA gene was amplified using primers 341 F (5'- CCTACGGGNGGCWGCAG- 3') and 805 R (5'- GACTACHVGGGTATCTAATCC- 3')<sup>16</sup>. For fungal community profiling, ITS1 region was amplified with ITS1-F (5'- TCGTCGGCAGCGTCAGATGTGTATAAGAGACAGCTTGGTCATTTAGAGGAAGTAA-3') and ITS1-R (5'- GTCTCGTGGGCTCGGAGATGTGTATAAGAGACAGGCTGCGTTCTTCATCGATGC-3')<sup>17</sup> and used for library preparation. Following indexing PCR,

amplified libraries were purified using KAPA HyperPure Beads (Roche; Cat. No. 8963851001) at a  $1.0 \times$  bead-to-sample ratio according to the manufacturer's instructions. The beads were equilibrated to room temperature, added to the sample, and mixed thoroughly to allow binding during the ten min incubation. The beads were then separated on a magnetic stand, the supernatant was discarded, and the pellet was washed twice with 80% ethanol. Air-dried, and libraries were eluted in nuclease-free water. The purified amplicon libraries were then quantified using Qubit 4 Fluorometer, and fragment size distribution was assessed using the Agilent 2100 Bioanalyzer with a high-sensitivity DNA kit (Cat. No. 5067 – 4626), following the manufacturer's instructions. After obtaining the mean peak size from the Tape station profile, the QC-passed libraries were sequenced on the Illumina MiSeq platform ( $2 \times 300$  bp paired-end mode) at Nucleome Informatics Private Limited (Hyderabad).

### Bioinformatics analysis

Raw reads were evaluated for quality using the FastQC tool (v0.12.1) under default settings. Parameters such as Phred quality score ( $> 30$ ), GC content, base composition, adapter dimers, and ambiguous bases were checked. Subsequently, sequences were processed in the Quantitative Insights into Microbial Ecology pipeline (QIIME2™ version 2025.7)<sup>18</sup>. Demultiplexed paired-end reads were merged, filtered, and denoised using the Divisive Amplicon Denoising Algorithm 2 (DADA2) plugin to generate representative amplicon sequence variants (ASVs). Taxonomic assignment of prokaryotic ASVs was carried out with a naïve Bayes classifier trained against the SILVA reference database (v138.1) at 99% sequence similarity to achieve higher taxonomic resolution for 16 S rRNA gene sequences generated through ASV-based pipelines<sup>19</sup>. Fungal ASVs were classified using the UNITE database (v10.0) with the naïve Bayes classifier with a confidence threshold of 99%<sup>20</sup>. Non-target sequences (non-bacterial or non-fungal) were filtered out prior to downstream analyses<sup>21</sup>. Community composition was visualised with bar plots. The  $\alpha$ -diversity measures, viz., number of taxa, Simpson Index, Shannon Index, Chao-1, abundance-based Coverage Estimator (ACE), dominance, evenness, and equitability were calculated in QIIME2 using the core metrics pipeline. Linear Discriminant Analysis Effect Size (LEfSe) was performed using the MicrobiomeAnalyst 2.0 to identify taxa that significantly discriminated among depth groups<sup>22</sup>. The analysis was conducted with default parameters: a Kruskal-Wallis  $\alpha$ -value of 0.05, a Wilcoxon  $\alpha$ -value of 0.05, and an LDA score threshold of 2.0 to determine discriminative features. Significant taxa were visualised using LDA score bar plots. Further, core microbial taxa were also identified using the MicrobiomeAnalyst 2.0. The total-sum scaled (TSS) abundance table was used as input, following data filtering (minimum count of 4 and prevalence in at least 20% of samples). Core taxa were defined based on a minimum relative abundance threshold of 0.1% and presence in  $\geq 70\%$  of samples within each group, following commonly applied prevalence-based thresholds for defining core microbiomes<sup>23,24</sup>. The resulting core microbiome was visualized through the bar plots generated within MicrobiomeAnalyst 2.0.

### Statistical analysis

The Shapiro-Wilk and Levene tests were used to determine the normality and homogeneity of variance. One-way ANOVA followed by post hoc analysis through Tukey's HSD test was used to compare the 'normal' data across different groups. The data lacking normality was log<sub>10</sub> transformed, and normality was rechecked. The data still lacking normality was checked by the Kruskal-Wallis H test. SPSS version 23 (SPSS, Chicago, USA) was used for the analysis. Principal Coordinate Analysis (PCoA) based on the Bray-Curtis similarity index of the ASV abundance profiles was performed to compare the microbiome data between different groups using Past 4.10 software<sup>25</sup>. The statistical significance of the clustering pattern revealed through the PCoA was checked using one-way permutational multivariate analysis of variance (PERMANOVA) based on the Bray-Curtis similarity index, and  $F$ -values and  $P$ -values were noted. Levins' niche breadth was calculated for each ASV to assess ecological specialization. For that, the ASV abundance table was first converted to relative abundances across all samples using the decostand function from the vegan package (version 2.7.2) in R (version 4.5.0). Niche breadth values were standardised ( $B_A$ ) following Hurlbert guidelines<sup>26</sup>. The ASVs were classified based on the standardized niche breadth ( $B_a$ ) values, where lower values (0 to 0.3) indicate specialists with narrow ecological tolerance, intermediate values (0.3 to 0.7) represent taxa with moderate niche breadth, and higher values (0.7 to 1) correspond to generalists with broad ecological adaptability<sup>27</sup>. Further, three-set Venn diagrams were made using the ASV feature table in Python 3.13.3 (Venn package v0.1.3; Matplotlib v3.10.3). Kendall's tau correlations between the log-transformed data on the abundances of different taxa at different levels and their corresponding depth were calculated using PAST 4.10 software. In all tests, the differences were interpreted as significant at  $p$ -values  $\leq 0.05$  and  $p$ -values were adjusted for multiple comparisons using the Bonferroni correction. The plot representing the strength and significance of correlations was designed using the tidyverse package version 2.0.0<sup>28</sup> in R software (version 4.5.0). To estimate the contributions of ASV features from 500 m (source) to the sink communities (750 m and 1000 m), the 'Feast' (Fast expectation maximisation microbial source tracking) was performed using R software. The results in the 'Feast' were plotted using a 2D pie chart and are interpreted as indicative of community mixing and potential vertical connectivity. The beta nearest taxon index ( $\beta$ NTI) analysis was used to calculate relative contribution of deterministic processes to the microbial communities using the 'picante' package version 1.8.2 in 'R software'. The  $|\beta$ NTI| values  $> 2$  were interpreted as deterministic processes, and  $|\beta$ NTI|  $< 2$  were interpreted as stochastic processes. To identify the environmental variables that significantly influenced the microbial community structure, Canonical Correspondence Analysis (CCA) was done in 'R' using the vegan package (version 2.7.2). This analysis was calculated based on the transformed ASV counts and the original environmental variable data<sup>29</sup>. Before CCA, multicollinearity among environmental variables was assessed using correlation analysis. Kendall's tau correlation coefficients were calculated, and variables showing strong collinearity ( $|\tau| \geq 0.75$ ,  $p < 0.05$ ) were carefully evaluated. From each highly correlated pair, only one representative variable was retained. To further reduce redundancy and avoid overfitting, Variance Inflation Factors (VIF) were computed using the vif.cca function in 'R'. Variables with VIF values  $> 5$  were sequentially

removed until the variables in the model exhibited acceptable collinearity levels. A forward selection procedure was applied to identify the most significant environmental predictors explaining community variation using the ordiR2 step function in the vegan package, based on  $R^2$  and permutation tests ( $n = 999$ ), and only variables that significantly improved model fit ( $p < 0.05$ ) were retained. CCA was then performed using the cca function in vegan. The significance of the overall CCA model was assessed using permutation-based ANOVA (anova.cca, 999 permutations). The proportion of variance explained by the constrained axes was reported using  $R^2$  values. Ordination plots were generated to visualise the relationships among samples and environmental gradients.

## Results

### Physicochemical characteristics of the sampling sites and organic compositions of the sediments

Environmental parameters of the sampling sites, viz. temperature, conductivity, pressure, density, dissolved oxygen, oxygen saturation, and salinity varied significantly ( $p \leq 0.05$ ) with depth (Table 1). The chlorophyll concentration was below the detection limit across all the depths. pH was significantly similar ( $p = 0.07$ ) across sampling sites. Temperature (10.78 to 8.87 °C) and conductivity (3.93 to 3.75 S/m) decreased with increasing depth, whereas pressure (731 to 1259 dBar) and density (1029 to 1031 kg/m<sup>3</sup>) showed an increasing trend. Salinity (35.21 to 35.15 PSU) and DO (0.59 to 0.67 mg/L) showed a subtle change only across the studied gradients.

The sediment composition was dominated by carbon, followed by hydrogen > nitrogen and sulphur. Except for sulphur, all the other three elements were significantly ( $p \leq 0.05$ ) higher at 1000 m, while sulphur showed the maximum level at 500 m.

### Sequencing summary and data availability

A total of 5,999,520 raw reads of 16 S rRNA were obtained (Supplementary File, SF1). These reads were assigned to 8,879 distinct ASVs. Based on rarefaction analyses, each sample was normalised to a sequencing depth of 84,887 reads (SF2A). The resulting datasets have been deposited in the NCBI-Sequence Read Archive (SRA) under Bioproject PRJNA1345746 (Accession numbers: SRR35800462 to SRR35800470).

Similarly, a total of 9,929,160 raw reads of ITS were obtained, and the reads were assigned to 1,353 distinct ASVs (SF1). Rarefaction analyses normalised each sample to a sequencing depth of 172,241 reads (SF2B). The datasets have been deposited in the NCBI-SRA under the same Bioproject with Accession numbers: SRR35800839 to SRR35800847.

### Overall microbial diversity measures and community structure in the mesopelagic zone

This section summarizes overall microbial diversity and community patterns across all samples. Depth-related variations in community structure are examined separately in section “Depth-related variations in microbial diversity and community structure”. Overall, the mesopelagic sediment microbiome exhibited a diverse and rich community structure of prokaryotes, with ~1508 observed prokaryotic taxa (based on ASVs), 5.33 as Shannon (H) and 0.97 as Simpson (1-D) indices (Table 2). Whereas fungal diversity measures showed a moderately rich and diverse community structure with ~205 observed fungal taxa (based on ASVs), 3.58 as Shannon (H) and 0.89 as Simpson (1-D) indices. The comparison of diversity measures between prokaryotes and fungi showed significant differences, where prokaryotes showed ~7.34, 1.48, 7.36, and 7.38 times higher numbers of taxa, Shannon, Chao-1, and ACE measures than fungi.

Parameter	Depth (m)		
	500	750	1000
Temperature (°C)	10.78 ± 0.00	9.37 ± 0.00	8.86 ± 0.00
Conductivity (S/m)	3.93 ± 0.00	3.80 ± 0.00	3.75 ± 0.00
Pressure (dBar)	731.18 ± 0.51	1096.57 ± 0.71	1259.04 ± 0.58
DO (mg/L)	0.59 ± 0.00	0.57 ± 0.01	0.67 ± 0.00
pH	8.16 ± 0.00	8.01 ± 0.00	8.01 ± 0.01
Chl-Flourescence (mg/m <sup>3</sup> )	BDL		
Salinity (PSU)	35.21 ± 0.00	35.18 ± 0.00	35.15 ± 0.00
Density (kg/m <sup>3</sup> )	1029.24 ± 0.00	1030.60 ± 0.00	1031.17 ± 0.00
Oxsol (mg/L)	8.86 ± 0.00	9.14 ± 0.00	9.24 ± 0.00
N (%)	0.88 ± 0.03	0.88 ± 0.03	0.88 ± 0.03
C (%)	7.53 ± 0.10	8.06 ± 0.10	8.27 ± 0.15
H (%)	1.53 ± 0.11	1.64 ± 0.02	1.71 ± 0.03
S (%)	0.43 ± 0.38	0.16 ± 0.28	0.37 ± 0.04
Protein (mg/ml)	0.16 ± 0.00	0.16 ± 0.00	0.16 ± 0.00

**Table 1.** Environmental parameters of the sampling sites and organic compositions of the sediments. Abbreviations: BDL: Below Detectable Level; PSU: Practical salinity unit.

Diversity measures	16 S rRNA	ITS
Number of taxa	1508.89 ± 180.19	205.56 ± 85.41***
Simpson Index	0.97 ± 0.024	0.89 ± 0.1
Shannon Index	5.33 ± 0.40	3.58 ± 1.05***
Chao-1	1513.67 ± 181.17	205.64 ± 85.39***
ACE	1521.22 ± 181.36	205.99 ± 85.47***
Dominance	0.03 ± 0.02	0.10 ± 0.13
Evenness	0.15 ± 0.05	0.22 ± 0.10
Equitability	0.73 ± 0.05	0.68 ± 0.16

**Table 2.** Microbial  $\alpha$ -diversity measures in the mesopelagic zone. Abbreviations: rRNA: ribosomal RNA; ITS: Internal Transcribed Spacer; ACE: Abundance-based Coverage Estimator. Diversity indices from ITS data that differ significantly ( $p \leq 0.05$ ) from those of 16 S rRNA data are indicated by asterisks. Three asterisks denote a highly significant difference ( $p \leq 0.001$ ) based on the Mann-Whitney U test.

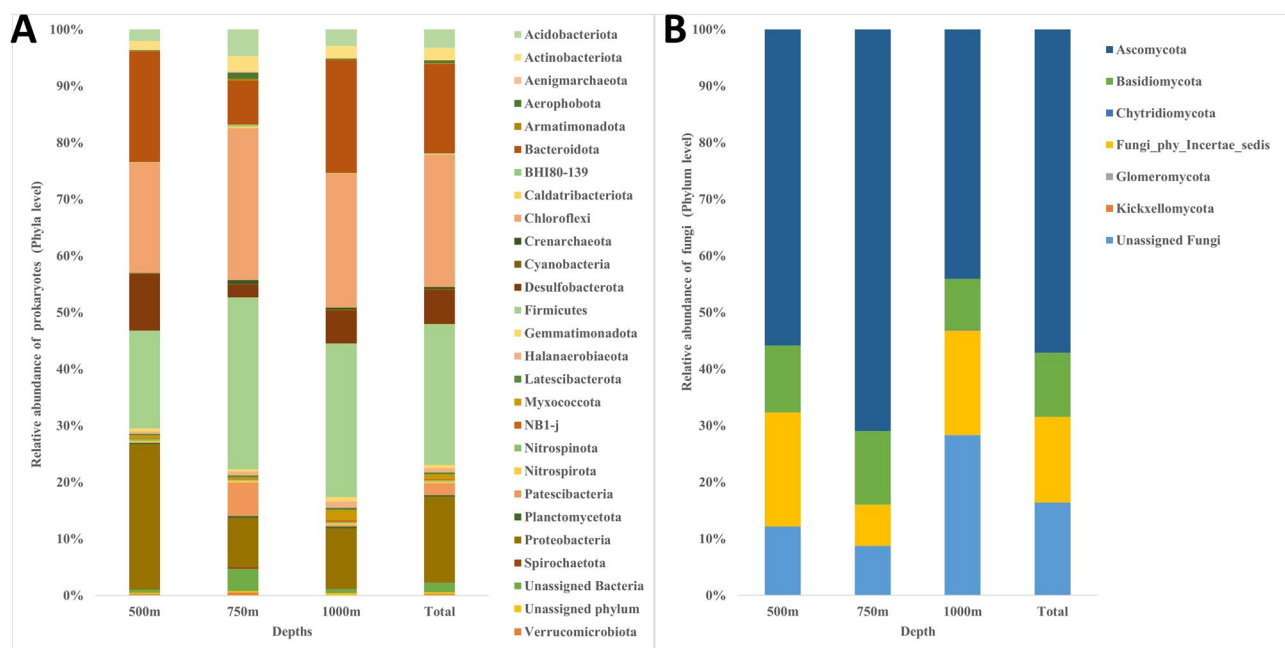


**Fig. 2.** Taxonomic landscape in the microbiome profiles across different depths.

**A:** Taxonomic landscape in the prokaryotic profiles at phylum level; **B:** Taxonomic landscape in the fungal profiles at phylum level. Taxa representing  $> 0.01\%$  of total abundance were only considered for making plots at phylum level.

Overall, taxonomic assignment of prokaryotes revealed 2 domains, 59 phyla, 133 classes, 274 orders, 390 families and 574 genera (SF3). At the domain level, Bacteria were the most abundant (99.09%), followed by Archaea. Overall, the most five abundant phyla included Firmicutes (17.2 to 27%), Chloroflexi (19.5 to 23.5%), Bacteroidota (19.5 to 19.8%), Proteobacteria (8.5 to 25.6%), and Desulfobacterota (2.3 to 10%) (Fig. 2A). The most abundant archaeal phylum was Crenarchaeota (0.4%) with 0.06%, 0.71%, and 0.38% abundance at 500, 750, and 1000 m, respectively. At the class level, Anaerolivia (16 to 21%) was consistently abundant, followed by Bacteroidia, Bacilli, Gamma-Proteobacteria, Clostridia, and Alpha-Proteobacteria. At the genus level, overall, uncultured *Anaerolinaceae* dominated (8 to 12%), followed by unassigned *Bacillaceae*, *Draconibacterium*, unassigned *Bacteroidia*, and *Magnetovibrio* (SF3). Analysis of the core microbiota revealed the members of the phyla Acidobacteriota, Bacteroidota, Chloroflexi, Firmicutes, and Proteobacteria as the major core microbes (500 to 1000 m depths) (Fig. 3A). At the genus level, overall, *Aminicentales* and *Draconibacterium* were the predominant core members (Fig. 3C; SF4).

Regarding fungal taxonomy, at the kingdom level, fungi (84.32%) were the most abundant at all depths, with relative abundances of 81%, 87%, and 85% at 500, 750, and 1000 m, respectively, while on average 15.06% remained as unassigned (SF3). At the phylum level, Ascomycota (48.17%) was the most abundant across all the depths. Overall, the three most abundant phyla included Ascomycota (37.02 to 61.88%), unassigned fungi (13.99 to 39.60%), Basidiomycota (7.68 to 11.31%), Chytridiomycota (0 to 0.06%) (Fig. 2B). Among the five top abundant genera, three remained unclassified (12.24% to 13.84%) followed by *Acremonium* (5.86%)

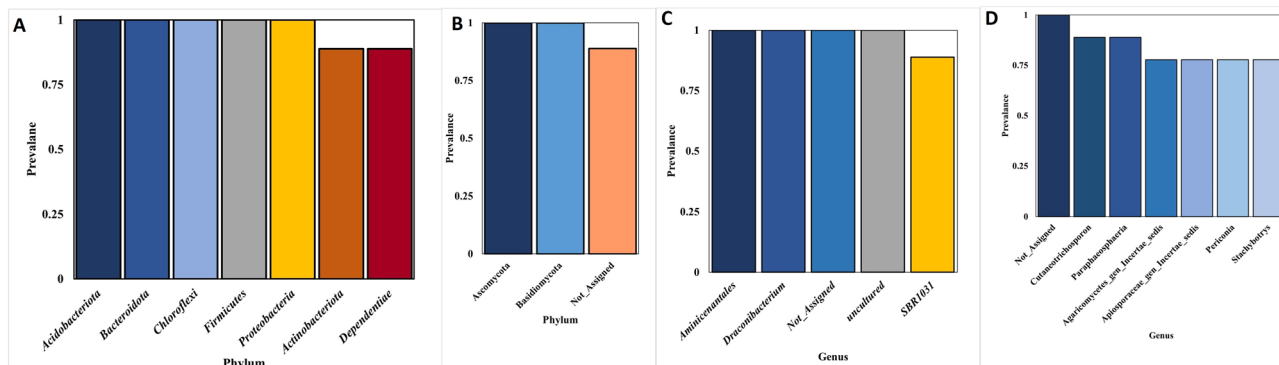


**Fig. 3.** Core microbial members of mesopelagic sediments. A: Core prokaryotes at phylum level; B: Core fungi at phylum level; C: Core prokaryotes at genus level; D: Core fungi at genus level.

Diversity measures	500 m	750 m	1000 m
16 S rRNA data			
Number of taxa	1409.67 ± 81.51 <sup>a</sup>	1570.67 ± 136.62 <sup>a</sup>	1546.33 ± 286.30 <sup>a</sup>
Simpson Index	0.9468 ± 0.03 <sup>a</sup>	0.98 ± 0.006 <sup>a</sup>	0.98 ± 0.007 <sup>a</sup>
Shannon Index	4.86 ± 0.28 <sup>a</sup>	5.56 ± 0.13 <sup>b</sup>	5.57 ± 0.26 <sup>b</sup>
Chao-1	1414.67 ± 83.42 <sup>a</sup>	1575 ± 139.08 <sup>a</sup>	1551.33 ± 287.25 <sup>a</sup>
ACE	1424 ± 85.75 <sup>a</sup>	1580 ± 139.27 <sup>a</sup>	1559.67 ± 288.58 <sup>a</sup>
Dominance	0.053 ± 0.03 <sup>b</sup>	0.020 ± 0.006 <sup>a</sup>	0.012 ± 0.007 <sup>a</sup>
Evenness	0.094 ± 0.03 <sup>a</sup>	0.17 ± 0.02 <sup>ab</sup>	0.17 ± 0.04 <sup>b</sup>
Equitability	0.67 ± 0.04 <sup>a</sup>	0.76 ± 0.016 <sup>b</sup>	0.76 ± 0.03 <sup>b</sup>
ITS data			
Number of taxa	273 ± 55.43 <sup>a</sup>	151.67 ± 109.44 <sup>a</sup>	192 ± 51.73 <sup>a</sup>
Simpson Index	0.98 ± 0.006 <sup>a</sup>	0.77 ± 0.156 <sup>a</sup>	0.96 ± 0.006 <sup>a</sup>
Shannon Index	4.471 ± 0.18 <sup>a</sup>	2.55 ± 1.23 <sup>ab</sup>	3.73 ± 0.24 <sup>b</sup>
Chao-1	273.03 ± 55.49 <sup>a</sup>	151.77 ± 109.42 <sup>a</sup>	192.13 ± 51.72 <sup>a</sup>
ACE	273.33 ± 55.67 <sup>a</sup>	152.02 ± 109.43 <sup>a</sup>	192.6 ± 52.02 <sup>a</sup>
Dominance	0.03 ± 0.007 <sup>a</sup>	0.23 ± 0.16 <sup>a</sup>	0.043 ± 0.006 <sup>a</sup>
Evenness	0.33 ± 0.06 <sup>a</sup>	0.11 ± 0.06 <sup>ab</sup>	0.22 ± 0.007 <sup>b</sup>
Equitability	0.80 ± 0.03 <sup>a</sup>	0.50 ± 0.18 <sup>ab</sup>	0.71 ± 0.01 <sup>b</sup>

**Table 3.** Depth-dependent changes in microbial diversity measures. Abbreviations: rRNA: ribosomal RNA; ITS: Internal Transcribed Spacer; ACE: Abundance-based Coverage Estimator, E: Evenness; Different alphabets in the superscripts indicate significantly different ( $p \leq 0.05$ ) values.

and *Paraphaeosphaeria* (5.04%). Analysis of the core microbiota revealed members of Basidiomycota and Ascomycota as core microbes (500 to 1000 m depths) (Fig. 3B; SF4). At the genus level, *Paraphaeosphaeria* and *Cutaneotrichosporon* were predominant core members across different depths (Fig. 3D).

Analysis for habitat generalists and specialists showed that 8484 prokaryotic ASVs were habitat specialists, 1093 intermediate specialists and 787 generalists (SF5). Of the generalists, the major ones include *Prevotella*, uncultured *Anaerolinaceae*, *JG30/KF-CM66*, *GIF3*, and *SBR1021*. Of the habitat specialists, 750 m contained the largest numbers (3373), followed by 1000 m (2706) and 500 m (2411). Regarding the fungal ITS data, we got 1368 ASVs as habitat specialists, 127 intermediate specialists and 22 generalists. Of the generalists, the major ones include unassigned fungi, *Paraphaeosphaeria* sp., *Acremonium sclerotigenum*, and *Periconia cortaderiae*. Of the habitat specialists, 500 m contained the largest numbers (603), followed by 1000 m (461) and 750 m (357) (SF5).

### Depth-related variations in microbial diversity and community structure

Vertical profiling revealed significant differences ( $p \leq 0.05$ ) in  $\alpha$ -taxonomics of both prokaryotic and fungal communities. In detail, 500 m sediments prokaryotes showed significantly higher dominance, but lower Shannon, evenness, and Equitability indices compared to 750 and 1000 m (Table 3). Other diversity measures however, remained similar across depths. PCoA showed three well-differentiated clusters in the prokaryotic profiles based on the depth gradients (Fig. 4A). The PERMANOVA test indicated a significant difference ( $p = 0.003$ ;  $F = 3.29$ ) of the clustering pattern revealed through the PCoA.

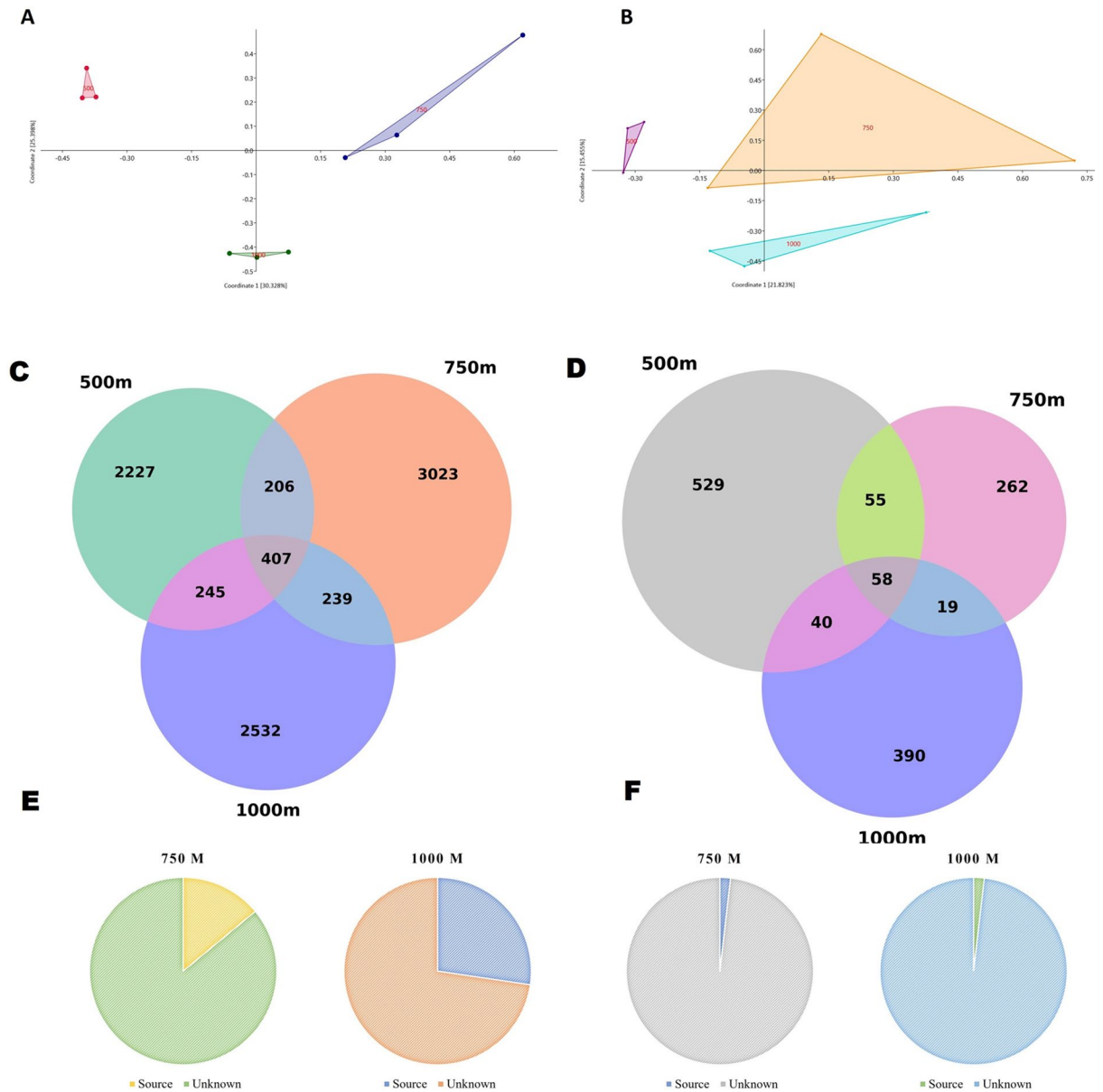


**Fig. 4.** Comparison of microbial taxonomic profiles between different depths. A: Principal coordinate analysis of profiles of prokaryotes based on Bray-Curtis similarity distances; B: Principal coordinate analysis of profiles of sediment fungi based on Bray-Curtis similarity distances; C: Shared prokaryotic ASVs between different depths; D: Shared fungal ASVs between different depths; E: Predictions using the ‘Feast microbial source tracking program’ to analyse vertical connectivity of prokaryotes from shallower (500 m) to deeper sediments (750 and 1000 m); F: Predictions using the ‘Feast microbial source tracking program’ to analyse vertical connectivity of fungi from shallower (500 m) to deeper sediments (750 and 1000 m). In Fig. C and D, the details of ASVs shared between each group are included in Supplementary File 6.

The trend in  $\alpha$ -taxonomics of fungal communities was opposite to that of prokaryotic communities. At 500 m, sediments exhibited higher Shannon, evenness, and Simpson values but lower dominance compared to 750 and 1000 m sediments (Table 3). Other diversity measures remained similar across depths. PCoA based on Bray-Curtis similarity index showed three well-differentiated clusters in the whole larval microbiota profiles (Fig. 4B). The PERMANOVA test indicated the significant difference ( $p=0.03$ ;  $F=1.3$ ) of the clustering pattern revealed through the PCoA.

In the next step, we checked for differential microbes across depth gradients. The Venn diagram illustrated 407 shared ASVs of prokaryotes across all depths (Fig. 4C; SF6). Comparative analysis revealed significant ( $p<0.05$ ) depth-dependent shifts in 10 phyla, 16 classes, 22 orders, 27 families, and 27 genera, including notable changes in key abundance ratios such as Bacteria: Archaea (highest at 500 m) and Firmicutes: Bacteroidota (lowest at 500 m), Proteobacteria to Acidobacteriota (highest in 500 m), and Firmicutes to Desulfobacterota (lowest in 500 m) (SF1). The LEfSe analysis identified a total of 9, 18, 20, 20, and 20 taxa at phylum, class, order, family,

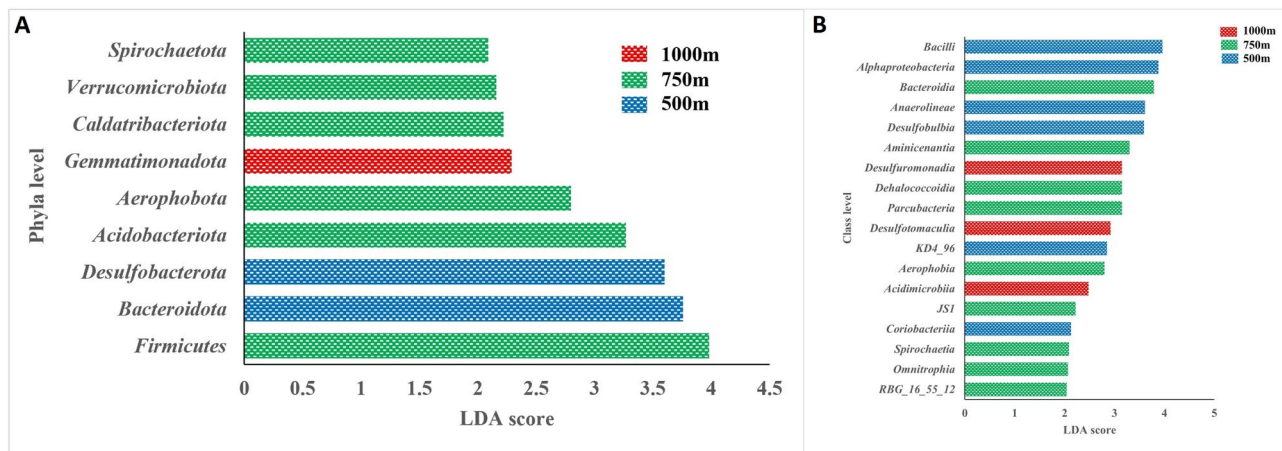


**Fig. 5.** Results of the linear discriminant analysis effect size (LEfSe) algorithm in the prokaryotic ASV profiles. A: At phylum level; B: At class level. The analysis was conducted with default parameters: a Kruskal-Wallis  $\alpha$ -value of 0.05, a Wilcoxon  $\alpha$ -value of 0.05, and linear discriminant analysis (LDA) score threshold of 2.0 to determine discriminative features.

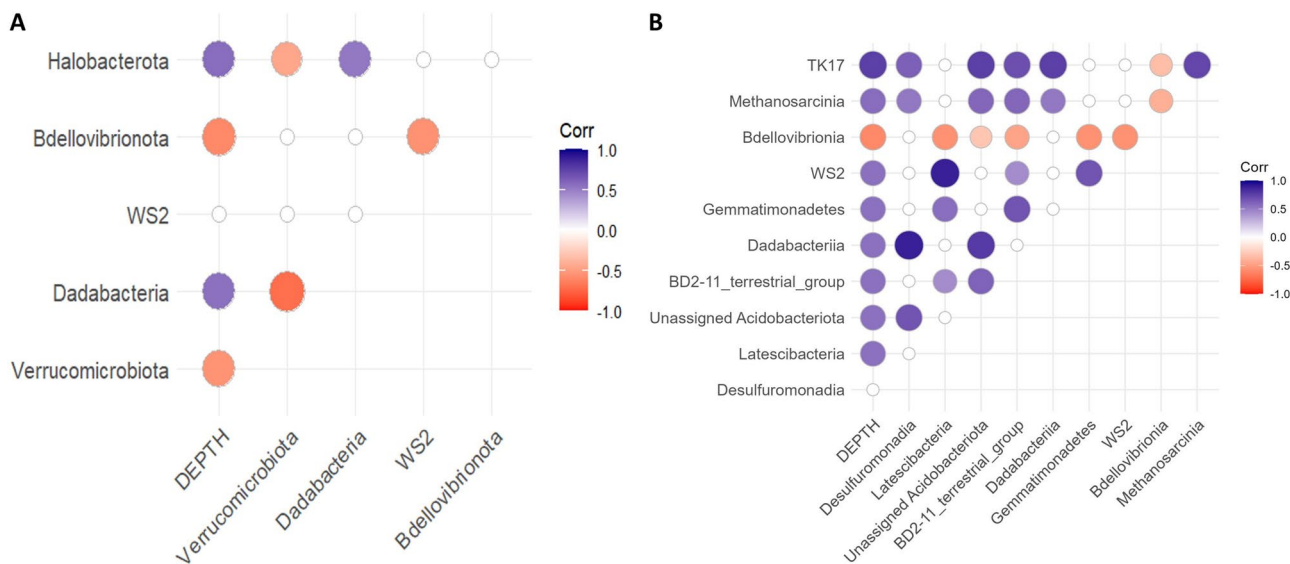


**Fig. 6.** Correlation analysis between the prokaryotic taxonomic profiles and depths in mesopelagic zone. A: At phylum level; B: At class level. Significant positive correlations ( $p \leq 0.05$ ) are indicated by blue bubbles and negative correlations are indicated by red bubbles. The size of bubbles indicates the strength of correlation. Details of correlations at order, family and genus level are included in Supplementary File 8.

genus levels as high-discriminating features between the three depths (Fig. 5A and B, and SF6). In particular, at the phylum level, Bacteroidota and Desulfobacteriota were the discriminating biomarkers at 500 m. Firmicutes and Acidobacteriota were the major discriminating biomarkers at 750 m. Gemmatimonadota was the high-dimensional marker at 1000 m (Fig. 5A).

Regarding the fungal ASVs, the Venn diagram illustrated 53 shared ASVs across all depths (Fig. 4D; SF7). Comparative analysis revealed significant ( $p < 0.05$ ) depth-dependent shifts in 2 phyla, one class, 3 orders, 4 families, and 8 genera. Further, there was a significant change in key abundance ratios such as Chytridiomycota to Ascomycota and Chytridiomycota to Basidiomycota ( $p = 0.02$ ) across different depths (SF1). However, the LEfSe analysis could not identify any significant discriminating ASV features between the three depths.

Correlation analysis between depth and the relative abundance of prokaryotic taxa revealed certain significant ( $p < 0.05$ ) positive and negative associations (Fig. 6A-B, SF8). At the phylum level, depth showed significant positive correlations with Dadabacteria and Halobacterota, and negative correlations with Verrucomicrobiota, WS2, and Bdellovibrionota. At the class level, significant positive correlations were observed for eight classes, while Bdellovibrionota showed a significant negative correlation (Fig. 6B). At the genus level, the strongest

positive correlations were observed for *Dehalobium*, uncultured *Anaerovoracaceae*, and *Lutibacter*, while three strongest negative correlations were for *Magnetovibrio*, *Pseudomonas* and unidentified *Lentimicrobiaceae* (SF8).

Regarding fungal taxa, the correlation analysis revealed certain significant ( $p < 0.05$ ) positive and negative associations (Fig. 7). At the phylum level, Chytridiomycota showed strong positive correlations with depth. At order level, only Sordariomycetes had a significant negative correlation with depth. At the genus level, the strongest negative correlations were observed for *Alfaria*, unidentified *Sordariomycetes*, and unidentified *Xylariales* (SF8).

### Microbial community assembly processes in deep-sea sediments

$\beta$ -NTI analysis of prokaryotic community structure indicated that all samples, except S4 ( $\beta$ NTI = 1.59), had  $|\beta$ NTI| > 2, suggesting that deterministic processes governed community assembly in 88.9% of the cases, while stochastic processes contributed only 11.1% of prokaryotic community variation. In fungal community, all samples, except S4 ( $\beta$ NTI = 1.65) and S5 ( $\beta$ NTI = 1.61), had  $|\beta$ NTI| < 2, suggesting that deterministic processes governed community assembly in 77.8% of the cases, while stochastic processes contributed only 22.2% of community variation.

FEAST analysis on the bacterial communities showed that 750 m and 1000 m sediments received only 14% and 27.33%, respectively, of their composition from 500 m, while the remaining fractions originated from unknown sources (Fig. 4E). No significant difference was observed between the contributions from 500 m to 750 and 1000 m communities ( $p = 0.66$ ). For fungal communities also, FEAST analysis revealed a similarly low contribution from 500 m to 750 and 1000 m sediments, with the majority of taxa originating from unknown sources (98.3% and 98% in 750 and 1000 m) (Fig. 4F). No significant difference was detected between the contributions from 500 m to 750 and 1000 m fungal communities ( $p = 0.2$ ).

### Explanatory power of geological factors and environmental factors

Correlation analysis of the variables revealed strong correlations among several predictors (SF1). Accordingly, a reduced set of environmental parameters (nitrogen, hydrogen, sulphur, protein, salinity, temperature, DO and pH) was retained for ordination. Forward selection identified (temperature, DO,  $N_2$ , and S) as significant predictors ( $p < 0.05$ ) and the model retaining these variables was significant ( $p = 0.011$ ). The CCA revealed that environmental variables explained 54.7% of the variation in prokaryotic community composition. The first two canonical axes (CCA1 and CCA2) accounted for 31.32% and 27.35% of the variance, respectively, cumulatively explaining 58.67% of the total variation in the dataset (Fig. 8A). The  $R^2$  and adjusted  $R^2$  of the model were 0.547 and 0.09, respectively. Of the different environmental variables, temperature ( $p = 0.013$ ) and DO ( $p = 0.002$ ) were the significant influencers of the community composition (Table 4).

Regarding the fungal community, the forward selection identified temperature,  $H_2$ ,  $N_2$ , and protein as significant predictors ( $p < 0.05$ ). The final model retaining these variables was significant ( $p = 0.03$ ). The environmental variables explained 52.1% of the variation in fungal community composition. The first two canonical axes (CCA1 and CCA2) accounted for 27.45% and 24.99% of the variance, respectively, cumulatively explaining 52.43% of the total variation in the dataset (Fig. 8B). The  $R^2$  and adjusted  $R^2$  of the model were 0.52 and 0.03, respectively. Of the different environmental variables, temperature ( $p = 0.04$ ) and  $N_2$  ( $p = 0.015$ ) were the significant influencers of the community composition (Table 4).

### Discussion

There are no prior studies on the depth-related patterns targeting both prokaryotic and fungal communities in the sediments of the mesopelagic zone, one of the most highly diverse, ecologically significant, but understudied areas of the ocean<sup>30</sup>. The present study provided detailed insights into microbial biodiversity and community

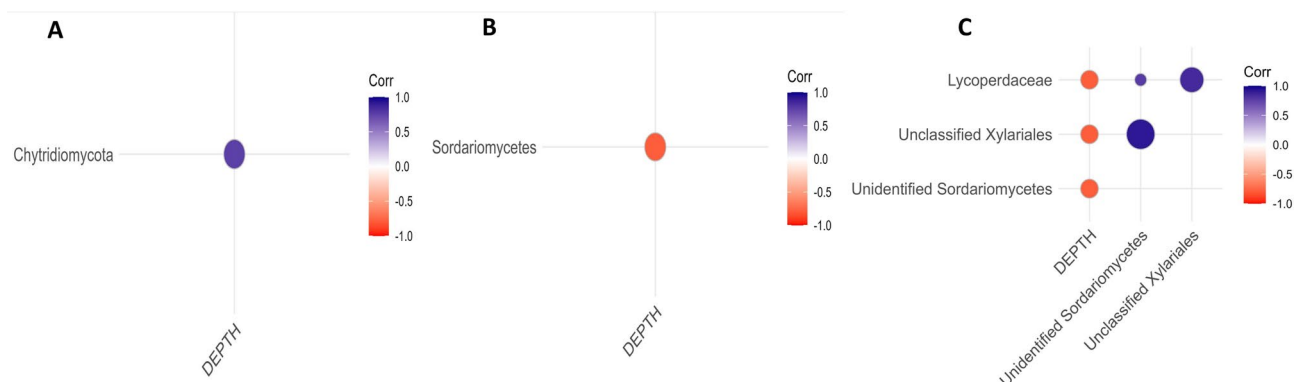


**Fig. 7.** Correlation analysis between the fungal taxonomic profiles and depths in mesopelagic zone. A: At phylum level; B: At order level; C: At family level. Significant positive correlations ( $p \leq 0.05$ ) are indicated by blue bubbles and negative correlations are indicated by red bubbles. The size of bubbles indicates the strength of correlation. No significant correlations were found between the fungal taxonomic profiles at class level and depth.

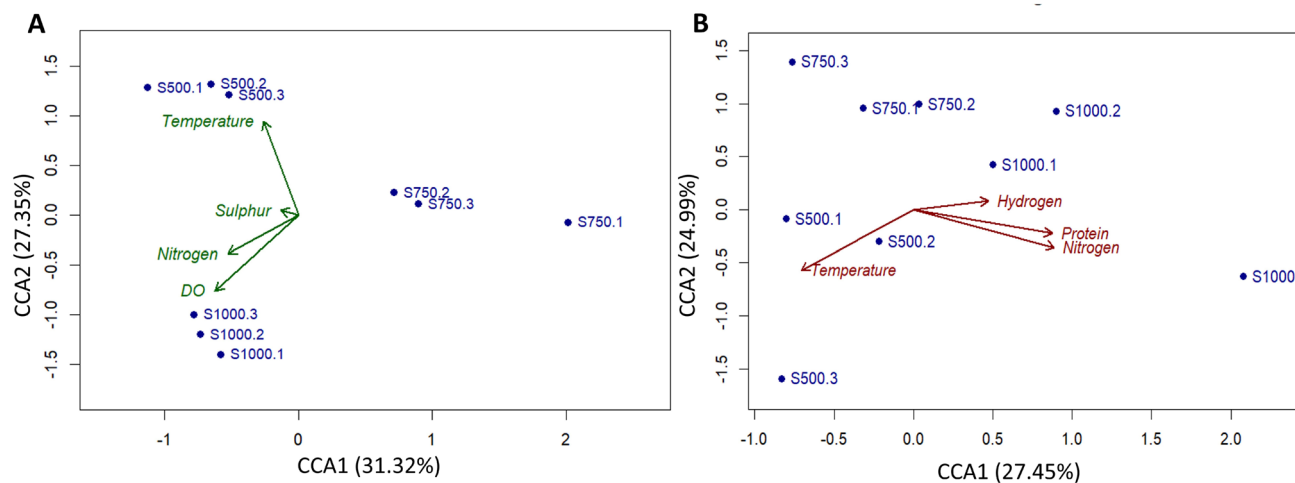


**Fig. 8.** Explanatory power of geological factors and environmental factors on microbiome profiles of mesopelagic sediments. A: Canonical correspondence analysis (CCA) of the prokaryotic community composition; B: CCA of the fungal community composition. Each blue point represents a sample, while arrows indicate environmental gradients influencing community composition/diversity measure. Arrow length and direction denote the strength and orientation of correlations with the CCA axes. The number markings of blue point indicate the depth and sample number in each depth.

Environmental variable	Chi-square	F-value	p-value
Prokaryotic community composition			
Temperature	0.57648	1.3270	0.01 *
DO	0.63494	1.4616	0.002 **
Nitrogen	0.40106	0.9232	0.73
Sulphur	0.48863	1.1248	0.23
Fungal community composition			
Temperature	0.70604	1.1312	0.04 *
Hydrogen	0.65428	1.0483	0.39
Nitrogen	0.70298	1.1263	0.01 *
Protein	0.65298	1.0462	0.28

**Table 4.** Permutation-based ANOVA of canonical correspondence analysis (CCA) showing the influence of environmental variables on marine microbial community. Significance codes:  $p \leq 0.01$  ‘\*\*’;  $p \leq 0.05$  ‘\*’ 0.05. Abbreviations: DO: Dissolved oxygen.

assembly processes in the upper continental slope sediments within the mesopelagic depth range ( $\geq 500$  m depth) of the Lakshadweep.

### Mesopelagic sediments harbour a rich and diverse microbiome, with marked distinctions across bathymetric gradients

The observed richness and diversity indices of both prokaryotic and fungal communities were higher than those reported for mesopelagic communities in the Southern Gulf of Mexico and Arctic marine sediments<sup>31,32</sup>, highlighting the comparatively higher biodiversity of the Lakshadweep deep-sea environment. Furthermore, diversity measures recorded in this study exceeded those from abyssal and hadal sediments<sup>11,33</sup>, likely reflecting the relatively milder environmental constraints at mesopelagic depths, leading to phylogenetically diverse microbial populations. The prokaryotic community structure exhibited higher diversity measures than the fungi. The lack of earlier studies directly comparing prokaryotic and fungal diversity measures within the same mesopelagic ecosystem limits cross-referencing with previous findings. However, the predominance of prokaryotes is consistent with their well-established metabolic versatility and dominant role as major agents of particulate organic matter remineralisation and nitrogen and sulfur cycling in mesopelagic zones<sup>34</sup>. In contrast, fungal communities in marine sediments are generally less diverse and are primarily associated with the degradation of complex organic substrates. The comparatively higher prokaryotic diversity suggests that prokaryotes are the principal drivers of nutrient transformation and microbial-mediated ecosystem functioning in mesopelagic sediments and underscores the distinct ecological roles and adaptive strategies of bacteria and fungi under varying mesopelagic environments.

Bacteria dominated (~ 99%) over archaea across mesopelagic depths, consistent with earlier observations from various mesopelagic habitats<sup>3,32</sup>. The consistent presence of archaea in all samples at all the analysed depths (500 to 1000 m) suggests that, despite their minor representation, archaeal populations may fulfill specialized ecological functions in the mesopelagic sediments. Among archaea, Crenarchaeota were the most abundant, consistent with their known dominant distribution in > 150 m depth in the Pacific Ocean and they might contribute to ammonia oxidation and nitrogen cycling under mesopelagic conditions<sup>35</sup>. A total of 62 phyla were detected, reflecting phylogenetically diverse prokaryotic communities adapted to mesopelagic sediment conditions. Among them, the most dominant phyla corroborate previous reports from mesopelagic sediment microbiomes and mesopelagic animal gut microbiomes<sup>3,30,32</sup>, indicating their ubiquity in the mesopelagic region of the deep sea. The consistent presence of Chloroflexi and Bacteroidota throughout mesopelagic zones has been well-documented, suggesting their involvement in the degradation of complex and recalcitrant organic substrates, including algal-derived biomass<sup>36</sup>. The core microbe feature of Acidobacteriota and dominance of Desulfobacterota might indicate the nitrate and nitrite conversion and sulphate reduction in mesopelagic zones<sup>37</sup>. Further, the core and dominant feature of Proteobacteria, a phylum encompassing diverse chemoheterotrophic and sulfur- and nitrogen-cycling taxa, likely show their pivotal roles in maintaining biogeochemical stability of mesopelagic zones<sup>38</sup>. At the genus level, the predominance of uncultured *Anaerolinaceae* and many unclassified genera underscores the presence of yet-uncharacterized microbial taxa in the mesopelagic sediments.

Ascomycota, followed by Basidiomycota, were the most abundant and core fungal phyla, consistent with observations from other marine sediment studies<sup>32,39</sup>. A substantial proportion of unassigned fungal sequences (13.99 to 39.60%) highlights the Lakshadweep deep-sea sediments as potential reservoirs of novel uncharacterized fungal taxa. The dominance of Ascomycota in the marine sediments was attributed to their metabolic potential for the degradation of refractory organic matter and involvement in carbon cycling<sup>2</sup>. Although Basidiomycota were less abundant in the present study, their consistent presence indicates an active role in complex polymer degradation as previously hypothesized<sup>40</sup>. The consistent detection of Chytridiomycota in deeper sediments (1000 m) coincides with the earlier report<sup>41</sup>. At the genus level, *Acremonium* and *Paraphaeosphaeria* were dominant, which are reported from marine environments as prolific producers of bioactive metabolites<sup>42</sup>. Overall, the prokaryotic and fungal community features observed in this study underscore the diversity and taxonomic heterogeneity of mesopelagic microbial assemblages in the Lakshadweep region.

Significantly differed prokaryotic community structures have been reported across vertical gradients in sediments from the Atlantic, Pacific, and Indian Oceans during the Malaspina expedition<sup>43</sup>. However, knowledge regarding the vertical variation of microbial communities within the upper continental slope sediments within the mesopelagic depth range remains limited<sup>43</sup>. Recently, Sun et al.<sup>9</sup> observed a distinct vertical distribution pattern for mesopelagic bacteria associated with protists in the South China Sea. Our results also showed a significant difference in the  $\alpha$  and  $\beta$  diversity measures across the studied depths, with prokaryotic and fungal communities responding differently to vertical gradients. Prokaryotic diversity measures at 500 m had a higher dominance, lower diversity and evenness measures, but similar richness, indicating that 500 m harbored a community dominated by a few specialized taxa. In contrast, fungal communities at 500 m exhibited a higher diversity and evenness with lower dominance and similar richness measures, suggesting a more evenly distributed assemblage with no single taxon dominating. The significantly similar richness across different vertical gradients for both prokaryotes and fungi suggests that differences in diversity are mainly driven by changes in relative abundances rather than loss or gain of taxa. Further, the contrasting results of prokaryotes and fungi may reflect differences in their ecological roles and adaptive strategies. There are both concordant and discrepant reports for our results. Generally, in marine systems, including the North Pacific Ocean<sup>44</sup>, Southern Gulf of Mexico<sup>33</sup>, and New Britain Trench<sup>45</sup>, bacterial and fungal diversity were reported to decline with depth, similar to our fungal results, attributed to reduced nutrient and energy availability. Conversely, our prokaryotic diversity patterns are consistent with observations from Atlantic sediments, where diversity and richness decreased in mesopelagic layers but increased in bathypelagic zones<sup>46</sup>. Similarly, Robinson et al.<sup>47</sup> recorded an increasing microbial diversity along with depth in the mesopelagic zone. For fungal communities, Rojas-Jimenez et al.<sup>48</sup> have reported minimal or inconsistent depth (380 to 3,474 m) effects on community composition, highlighting the context-dependent nature of microbial ecology in marine sediments. These differences underscore the importance of investigating the site-specific environmental and sedimentological contexts in shaping the microbial community of marine sediments along with bathymetric gradients.

Analysis for habitat generalists and specialists again showed that the majority of prokaryotic and fungal ASVs were classified as habitat specialists, suggesting a strong influence of vertical and environmental heterogeneity. Zhou et al.<sup>49</sup> showed that sediment communities of a large shallow lake contained more specialists, while the water samples contained more generalists. Venn diagram also revealed a mixture of generalists and depth-restricted microbial taxa with a substantial number of depth-specific ASVs, again highlighting the distinct depth-mediated selection pressures driving sediment microbial niche differentiation. The presence of habitat specialists and shared ASVs across all depths also suggested a stable microbiome persisting throughout the vertical gradients in the mesopelagic sediments. Briefly, while a stable microbiota is present across different depths to maintain essential ecological functions, there are more depth-specific specialists, suggesting that environmental heterogeneity and depth-related gradients promote niche specialisation. However, a limited number of samples and the presence of low-abundant taxa may influence niche breadth estimates, potentially inflating the proportion of habitat specialists. Therefore, while the observed pattern may reflect both ecological specialisation and methodological constraints, further studies with greater sample sizes are required to validate these trends.

Given the pronounced compositional differences of mesopelagic sediment microbial communities across the depth gradients, the ASVs specific to each depth layer were examined. Comparative analysis revealed significant depth-dependent shifts in 16 prokaryotic phyla, along with conforming variations across multiple

taxonomic levels. At the same time, balanced distribution of Chloroflexi in the upper and lower mesopelagic zone was reported, supporting our results<sup>50</sup>. Most importantly, bacterial abundance decreased with depth, with corresponding increase in Archaea consistent with the report from the North Pacific Ocean<sup>44</sup>. We also identified significant changes in key abundance ratios, such as Bacteria: Archaea, Firmicutes: Bacteroidota, Proteobacteria: Acidobacteriota and Firmicutes: Desulfobacterota, indicating shifts in energy utilisation strategies. The higher Bacteria: Archaea ratio at shallower sediments supports the previous hypothesis on the dominance of heterotrophic bacterial processes in upper and transition to chemolithoautotrophic Archaea in deeper mesopelagic zones<sup>51</sup>. The increase in the relative abundance of Archaea, especially Crenarchaeota, along with an increase in depth, is reported in other marine ecosystems<sup>36</sup>. Similarly, the increased Proteobacteria: Acidobacteriota and decreased Firmicutes: Desulfobacterota ratio at upper zones is consistent with enhanced microbial respiration and organic matter remineralisation near the upper mesopelagic zones<sup>52</sup>. The LEfSe analysis identified multiple high-dimensional differential biomarkers between depths, reflecting taxonomic specialisation and metabolic adaptation along depth gradients. In contrast, the fungal community exhibited a lower degree of compositional differentiation across depths. Absence of statistically significant discriminating ASV features in LEfSe analysis further supports the concept that fungal communities are more stable and less sensitive to depth-related gradients than prokaryotic counterparts. However, the significant changes in the ratios, like Chytridiomycota: Ascomycota and Chytridiomycota: Basidiomycota ratios, suggest shifts in organic matter degradation potential, with Chytridiomycota favouring recalcitrant carbon compounds in deeper sediments and Ascomycota utilising more labile organic substrates in shallower layers<sup>11,53</sup>.

The correlation analysis between depth and the relative abundance of microbial taxa revealed clear stratification patterns, with several taxa exhibiting significant positive or negative associations along the depth gradient. Certain significant correlations like negative correlations of Rhodospirillales and Bdellovibrionaceae with depth in the mesopelagic zone, were reported earlier<sup>50</sup>. Compared to prokaryotic communities, the extent of depth influence was less for fungal communities. At the phylum level, Chytridiomycota showed a strong positive correlation with depth, consistent with the findings of Nagano et al.<sup>54</sup>. Overall, these findings collectively suggest that depth stratification exerts stronger selective pressure on prokaryotic communities, leading to distinct taxonomic and functional profiles, while fungal communities remain comparatively conserved but still exhibit depth-associated compositional differences.

### Deterministic processes appeared to play a significant role in shaping the microbial community with limited vertical connectivity

The FEAST analysis showed that the majority of microbial taxa of deeper layers originated from unknown sources and only a small portion originated from 500 m, emphasising the limited vertical connectivity from shallower regions to deeper sediments, consistent with observations of predominance of habitat specialists. It is important to note that FEAST analysis is primarily as a microbial source tracking tool and was employed in the present study to estimate the contribution of microbial communities from 500 m to 750 and 1000 m sediment depths, providing insights into potential vertical connectivity and source-sink relationships rather than direct evidence for ecological dispersal processes. Similar applications have been reported in habitat-based microbial studies<sup>48</sup>, although such interpretations remain inferential. Zhou et al.<sup>49</sup> observed a low vertical connectivity in sediment bacteria but a higher exchange in water column communities, aligning with our results. The  $\beta$ -NTI analysis suggested a greater influence of deterministic processes than stochastic processes on microbial communities in mesopelagic sediments. Conversely, Qu et al.<sup>55</sup> found that stochastic processes primarily drive fungal community assembly in river sediments, likely reflecting ecosystem differences. Collectively, the analyses on diversity metrics, habitat specialists, FEAST source tracking, and  $\beta$ -NTI analyses highlight that both prokaryotic and fungal communities exhibit depth-specific ecological structuring with limited vertical connectivity, reflecting the combined influence of depth gradients, environmental filtering, niche differentiation, and localised recruitment in mesopelagic sediments.

### Environmental and sedimentological drivers of microbial community structure in mesopelagic sediments

Environmental parameters of the sampling sites exhibited clear depth-related trends, reflecting the physical and chemical stratification typical of mesopelagic sediments. Temperature and conductivity decreased with depth, whereas pressure and density increased, consistent with standard oceanographic profiles of mesopelagic zones<sup>47</sup>. DO showed a non-linear pattern, being lowest values at 750 m. The pH remained relatively constant across the gradients, and chlorophyll was below detection limits across all depths. Regarding the sediment composition, carbon-dominated, followed by hydrogen, nitrogen, and sulfur, reflecting typical marine sediment elemental distributions<sup>56</sup>. The carbon, hydrogen, and nitrogen concentrations were significantly higher at 1000 m, suggesting sedimentation of hard-to-degrade organic matters or selective preservation under low-energy conditions<sup>57</sup>. The progressive decrease in sulphur may be due to the progressive sulfur depletion or enrichment of refractory organic carbon in deeper sediments<sup>58</sup>. Collectively, these observations indicate that the mesopelagic environment of the Lakshadweep region exhibits well-defined vertical gradients in both physicochemical and geochemical parameters as reported for other areas<sup>47</sup>. Such gradients are likely to influence microbial community structure, which was explored in the next step.

The CCA analysis revealed that environmental variables and sediment organic composition exert control over the microbial community structure in the mesopelagic sediments. The CCA model incorporating temperature, DO, N<sub>2</sub>, and S was significant and explained 54.7% of the total variation in the prokaryotic community. Among the variables, DO and temperature were the significant drivers, suggesting that oxygen and thermal regimes play a pivotal role in shaping mesopelagic sediment bacterial community composition. The significant relationship between environmental parameters and prokaryotic community aligns with previous

findings in sea sediments<sup>45,59</sup>. Further, the role of environmental conditions, particularly temperature and oxygen availability, on zooplankton abundance of the mesopelagic zone was already established<sup>60</sup>, supporting our results. A similar association between prokaryotic community and hydrography in the Arctic mesopelagic sediments was reported<sup>61</sup>. Sun et al.<sup>50</sup> also reported the influence of temperature in driving the mesopelagic bacterial community associated with protists of the South China Sea. Similarly, significance of DO as a major driver of bacterial distribution in mesopelagic waters<sup>62,63</sup> was reported, supporting our results.

Regarding the fungal community the CCA model incorporating temperature, H<sub>2</sub>, N<sub>2</sub>, and protein explained 52.1% of the total variation, indicating a moderate but significant response of fungal community to environmental gradients. Among the variables, nitrogen content in the sediments and temperature were the major drivers of fungal community composition. Breyer et al.<sup>64</sup> recorded the active involvement of oceanic fungi in nitrogen degradation, supporting our results. Further, Lin et al.<sup>8</sup> showed that the fungal diversity of the estuarine sediments was significantly correlated with NH<sub>4</sub><sup>+</sup> concentrations. The significance of nitrogen content as a regulator of the marine fungal community of surface sediments was reported by Guo et al.<sup>65</sup>. Whereas Sun et al.<sup>50</sup> showed that the fungal community was only significantly influenced by temperature. Breyer and Baltar<sup>66</sup> in their meta-analysis listed temperature, depth, pH, salinity and the availability of C, N, and P as potential influencers on the fungal community of oceanic waters. Banchi et al.<sup>67</sup> emphasized that organic carbon and nitrogen were significant drivers of the fungal communities. Overall, these findings highlight that both bacterial and fungal community of mesopelagic sediments is significantly related to deterministic environmental variables, with DO and temperature as the major variables for prokaryotes and nitrogen contents and temperature as the major variables for fungi, underscoring the complex but structured nature of microbial community assembly across mesopelagic depth gradients in the Lakshadweep archipelago sediments.

### Limitations

Despite providing valuable insights, this study is constrained by a relatively small sample size ( $n=9$ , representing three depths with triplicate sediment replicates from each depth) due to the logistical challenges associated with sampling in deep-sea environments. While this sampling design is adequate for describing microbial community composition and broad depth-related patterns, it may limit the statistical robustness of multivariate and ecological inference analyses. Community assembly metrics ( $\beta$ NTI), source tracking (FEAST), and ordination-based models (CCA) can be sensitive to sample number and variable complexity. Therefore, the observed patterns are indicative rather than definitive, and further studies with expanded spatial and sampling coverage are required to validate these findings and strengthen ecological generalisations.

### Conclusion

The present manuscript provides novel insights into microbial (prokaryotic and fungal) diversity and community within mesopelagic sediments of the Lakshadweep Islands, an understudied tropical marine ecosystem. Predominant role of deterministic processes than stochastic effects suggests that environmental filtering plays a central role in structuring these communities. The limited vertical connectivity indicated pronounced niche differentiation along bathymetric gradients. Among ecological features analysed, DO and temperature were the primary determinants of prokaryotic assemblages, whereas nitrogen and temperature predominantly shaped fungal communities. Overall, the findings highlight the critical roles of depth-driven environmental heterogeneity in structuring microbial communities of mesopelagic sediments. In the context of growing anthropogenic pressures, climate-driven variations, and pollution on deep-sea ecosystems, identifying such depth-dependent and environmental microbial dynamics is important for predicting ecosystem effects and updating conservation policies. The findings contribute to a broader understanding of microbial ecology in tropical deep-sea systems and provide a foundation for future functional and temporal investigations.

### Data availability

Metagenomic sequencing data were placed in the NCBI-SRA (Sequence Read Archive) database under Bioproject PRJNA1345746 (Accession numbers: SRR35800462 to SRR35800470 for 16 S rRNA and SRR35800839 to SRR35800847 for ITS data).

Received: 2 January 2026; Accepted: 9 April 2026

Published online: 15 April 2026

### References

1. Varliero, G., Bienhold, C., Schmid, F., Boetius, A. & Molari, M. Microbial diversity and connectivity in deep-sea sediments of the South Atlantic polar front. *Front. Microbiol.* **10**, 665 (2019).
2. Zvereva, L. V. & Borzykh, O. G. Fungi in deep-sea ecosystems of the World Ocean: a review. *Russ J. Mar. Biol.* **48**, 139–148 (2022).
3. Chen, J. et al. Global marine microbial diversity and its potential in bioprospecting. *Nature* **633**, 371–379 (2024).
4. Rayne, R. R. P. et al. Temporal shifts in prokaryotic metabolism in response to organic carbon dynamics during a mesopelagic export event in the Southern Ocean. *Deep Sea Res. Part. II Top. Stud. Oceanogr.* **214**, 105368 (2024).
5. Baltar, F., Aristegui, J., Gasol, J. M. & Herndl, G. J. Microbial functioning and community structure variability in mesopelagic and epipelagic waters of the subtropical Northeast Atlantic Ocean. *Appl. Environ. Microbiol.* **78**, 3309–3316 (2012).
6. Zhang, Y., Liu, H. & Jing, H. Community differences and potential function along the particle size spectrum of microbes in the twilight zone. *Microbiome* **13**, 121 (2025).
7. Nagano, Y. et al. Cryptic fungal diversity revealed in deep-sea sediments associated with whale-fall chemosynthetic ecosystems. *Mycology* **11**, 263–278 (2020).
8. Lin, X. et al. Nitrogen mineralization and immobilization in surface sediments of coastal reclaimed aquaculture ecosystems. *Front. Mar. Sci.* **9**, 1093279 (2023).
9. Sun, P. et al. Seasonal patterns of mesopelagic protistan–bacterial microbiomes. *Prog Oceanogr.* **225**, 103280 (2024).

10. Lian, K. et al. Environmental gradients shape microbiome assembly and stability in the East China Sea. *Environ. Res.* **238**, 117197 (2023).
11. Li, Y. et al. Depth shapes microbiome assembly and network stability in the Mariana Trench. *Microbiol. Spectr.* **12**, e02110–e02123 (2024).
12. Mende, D. R., Boeuf, D. & DeLong, E. F. persistent core populations shape the microbiome throughout the water column in the North Pacific Subtropical Gyre. *Front. Microbiol.* **1** (10), 2273. <https://doi.org/10.3389/fmicb.2019.02273> (2019).
13. Ammanabrolu, B. S. & Dineshran, R. Unveiling diversity in inhabited and uninhabited reefs of the Lakshadweep archipelago, India using eDNA. *Front. Mar. Sci.* **12**, 1592429 (2025).
14. Kumbhare, S. V. et al. Diversity and imputed metabolic potential of bacterial communities in the continental shelf of Agatti Island. *PLoS ONE*. **10**, e0129864 (2015).
15. Lowry, O. H. et al. Protein measurement with the Folin phenol reagent. *J. Biol. Chem.* **193**, 265–275 (1951).
16. Klindworth, A. et al. Evaluation of general 16S rRNA gene PCR primers for diversity studies. *Nucleic Acids Res.* **41**, e1 (2013).
17. Zhernova, D. A. et al. ITS and 16S rDNA metagenomic dataset of soils from flax fields. *Data Brief.* **52**, 109827 (2024).
18. Bolyen, E. et al. Reproducible, interactive, scalable and extensible microbiome data science using QIIME 2. *Nat. Biotechnol.* **37**, 852–857 (2019).
19. Bokulich, N. A. et al. Optimizing taxonomic classification of marker-gene amplicon sequences with QIIME 2's q2-feature-classifier plugin. *Microbiome* **6** (1), 90. <https://doi.org/10.1186/s40168-018-0470-z> (2018).
20. Abarenkov, K. et al. The UNITE database for molecular identification and taxonomic communication of fungi and other eukaryotes: sequences, taxa and classifications reconsidered. *Nucleic Acids Res.* **52** (D1), D791–D797. <https://doi.org/10.1093/nar/gkad1039> (2024).
21. Bokulich, N. A. et al. Quality-filtering vastly improves diversity estimates from Illumina amplicon sequencing. *Nat. Methods.* **10**, 57–59 (2013).
22. Lu, Y. et al. MicrobiomeAnalyst 2.0. *Nucleic Acids Res.* **51**, W310–W318 (2023).
23. Singh, R., Haque, M. M. & Mande, S. S. Lifestyle-induced microbial gradients: an Indian perspective. *Front. Microbiol.* **10**, 2874 (2019).
24. Custer, G. F. et al. Comparative analysis of core microbiome assignments: Implications for ecological synthesis. *mSystems* **8** (1), e0106622. <https://doi.org/10.1128/msystems.01066-22> (2023).
25. Hammer, Ø. & Harper, D. A. PAST Paleontological statistics software package for education and data analysis. *Palaeontol. Electron.* **4**, 1 (2001).
26. Hurlbert, S. H. The measurement of niche overlap and some relatives. *Ecology* **59**, 67–77 (1978).
27. Adamczuk, M. Monitoring of diet and habitat preferences indicates competitive effect of exotic *Ictalurus nebulosus* on native fish under food-limited conditions. *Glob Ecol. Conserv.* **34**, e02060 (2022).
28. Wickham, H. et al. Welcome to the tidyverse. *J. Open. Source Softw.* **4**, 1686 (2019).
29. Borcard, D., Gillet, F. & Legendre, P. *Numerical Ecology with R 2* (Springer, 2018).
30. Breusing, C., Osborn, K. J., Girguis, P. R. & Reese, A. T. Composition and metabolic potential of microbiomes associated with mesopelagic animals from Monterey Canyon. *ISME Commun.* **2**, 117 (2022).
31. Zhang, T. et al. Diversity of fungal communities in Arctic marine sediments. *Sci. Rep.* **5**, 14524 (2015).
32. Osorio-Pando, L. S. et al. Meso- and bathypelagic microbial communities of the southern Gulf of Mexico. *Microorganisms* **13**, 1106 (2025).
33. Sunagawa, S. et al. Structure and function of the global ocean microbiome. *Science* **348**, 1261359 (2015).
34. Friedlingstein, P. et al. Global carbon budget 2022. *Earth Syst. Sci. Data.* **14**, 4811–4900 (2022).
35. Karner, M. B., DeLong, E. F. & Karl, D. M. Archaeal dominance in the mesopelagic zone of the Pacific Ocean. *Nature* **409**, 507–510 (2001).
36. Mo, J. et al. Prokaryotic diversity and community assembly in Arabian Sea sediments linked to mesopelagic hypoxia. *Mar. Environ. Res.* **2025**, 107237 (2025).
37. Tan, S. et al. Vertical distribution of bacterial communities in Bohai Sea sediments. *Sci. Nat.* **112**, 37 (2025).
38. Osorio-Pando, L. S. et al. The meso- and bathypelagic archaeal and bacterial communities of the Southern Gulf of Mexico are dominated by nitrifiers and hydrocarbon degraders. *Microorganisms* **13** (5), 1106. <https://doi.org/10.3390/microorganisms13051106> (2025).
39. da Silva, M. K. et al. Fungal and fungal-like diversity in marine sediments from the maritime Antarctic assessed using DNA metabarcoding. *Sci. Rep.* **12**, 21044 (2022).
40. Raghukumar, S. Marine fungal physiology and biotechnology. In *Fungi in Coastal and Oceanic Marine Ecosystems* (2017).
41. Vargas-Gastélum, L. & Riquelme, M. The mycobiota of the deep sea. *Life* **10**, 292 (2020).
42. Huo, R. et al. Halogenated meroterpenoids with antifungal activities from the deep-sea-derived fungus *Acremonium sclerotigenum*. *Bioorg. Chem.* **156**, 108186 (2025).
43. Ruiz-González, C. et al. Surface plankton imprint on deep ocean prokaryotes. *Mol. Ecol.* **29**, 1820–1838 (2020).
44. Brown, M. V. et al. Microbial community structure in the North Pacific Ocean. *ISME J.* **3**, 1374–1386 (2009).
45. Liu, K. et al. Macro- and microelements drive prokaryotic and fungal communities in hypersaline sediments. *Front. Microbiol.* **9**, 352 (2018).
46. Gómez-Letona, M. et al. Deep Ocean prokaryotes and fluorescent dissolved organic matter reflect the history of the water masses across the Atlantic Ocean. *Prog Oceanogr.* **205**, 102819 (2022).
47. Robinson, C. et al. Mesopelagic zone ecology and biogeochemistry. *Deep Sea Res. Part. II.* **57**, 1504–1518 (2010).
48. Rojas-Jimenez, K. et al. Fungal communities in sediments along a depth gradient. *Front. Microbiol.* **11**, 575207 (2020).
49. Zhou, T. et al. Assembly and network stability of bacterial communities in a shallow lake. *Ecol. Indic.* **177**, 113761 (2025).
50. Sun, D. et al. Seasonal and depth variations of pelagic microbial communities. *Deep Sea Res. Part. I.* **218**, 104463 (2025).
51. Zhou, Y. L. et al. Microbiomes in challenger deep sediments. *Nat. Commun.* **13**, 1515 (2022).
52. Aristegui, J., Gasol, J. M., Duarte, C. M. & Herndl, G. J. Microbial oceanography of the dark ocean's pelagic realm. *Limnol. Oceanogr.* **54**, 1501–1529 (2009).
53. Orsi, W., Biddle, J. F. & Edgcomb, V. Deep sequencing reveals active fungi in marine subsurface provinces. *PLoS ONE.* **8**, e56335 (2013).
54. Nagano, Y. et al. Fungal diversity in deep-sea sediments. *Fungal Ecol.* **3**, 316–325 (2010).
55. Qu, W., Zuo, Y., Zhang, Y. & Wang, J. Structure and assembly of fungal communities in the Yangtze River Estuary. *Front. Microbiol.* **14**, 1220239 (2024).
56. LaRowe, D. E. et al. The fate of organic carbon in marine sediments. *Earth-Sci. Rev.* **204**, 103146 (2020).
57. Zonneveld, K. A. F. et al. Selective preservation of organic matter in marine environments: processes and impact on the sedimentary record. *Biogeosciences* **7**, 483–511 (2010).
58. Roerdink, D. L. et al. Hydrothermal activity fuels microbial sulfate reduction. *Front. Mar. Sci.* **10**, 1320655 (2024).
59. Salazar, G. et al. Global diversity and biogeography of deep-sea pelagic prokaryotes. *ISME J.* **10**, 596–608 (2016).
60. Casas, L., Pearman, J. K. & Irigoien, X. Metabarcoding reveals seasonal and temperature-dependent succession of zooplankton communities in the Red Sea. *Front. Mar. Sci.* **4**, 241 (2017).
61. Galand, P. E., Potvin, M., Casamayor, E. O. & Lovejoy, C. Hydrography shapes bacterial biogeography of the deep Arctic Ocean. *ISME J.* **4**, 564–576 (2010).

62. Aldunate, M., De la Iglesia, R., Bertagnolli, A. D. & Ulloa, O. Oxygen modulates bacterial community composition in the coastal upwelling waters off central Chile. *Deep Sea Res. Part. II Top. Stud. Oceanogr.* **156**, 68–79 (2018).
63. Rigonato, J. et al. Ocean-wide comparisons of mesopelagic planktonic communities. *ISME Commun.* **3**, 83 (2023).
64. Breyer, E., Zhao, Z., Herndl, G. J. & Baltar, F. Global contribution of pelagic fungi to protein degradation in the ocean. *Microbiome* **10**, 143 (2022).
65. Guo, X. et al. Marine fungal communities in water and surface sediment of a sea cucumber farming system. *Fungal Ecol.* **14**, 87–98 (2015).
66. Breyer, E. & Baltar, F. The largely neglected ecological role of oceanic pelagic fungi. *Trends Ecol. Evol.* **38**, 870–888 (2023).
67. Banchi, E., Manna, V., Muggia, L. & Celussi, M. Marine fungal diversity and dynamics in the Gulf of Trieste (Northern Adriatic Sea). *Microb. Ecol.* **87**, 78 (2024).

## Acknowledgements

Authors express sincere gratitude to the Director, ICAR-CMFRI, Kochi for providing institutional support. Financial support from Ministry of Earth Sciences funded project on ‘Deep-sea Metagenomics for enhanced next-generation bioethanol production’ under deep ocean mission as research fellowship provided to VSM, NN and GS are also acknowledged. GS expressed her gratitude to the authorities at the CUSAT for granting her Ph.D. registration.

## Author contributions

Authors mutually agree to submit this paper for publication. TGS had the idea of article, supervised the project, analysed the data and drafted the manuscript. KSSR critically revised the manuscript. GS did the bioinformatics analysis and created figures presented in the manuscript. NN, VSM, ZAPM, and RKR are involved in the sampling. AVN and LR provided technical assistance in the sample analysis. DB and KRS assisted during manuscript preparation. All authors have analysed and approved the final version of manuscript to be submitted.

## Funding

This study was supported by Ministry of Earth Sciences funded project on ‘Deep-sea Metagenomics for enhanced next-generation bioethanol production’ under Deep Ocean Mission (DOM) [MoES/PAMC/DOM/176/2023 (E-14624)] and Indian Council of Agriculture Research, Department of Agriculture, Research and Education, Government of India.

## Competing interests

The authors declare no competing interests.

## Additional information

**Supplementary Information** The online version contains supplementary material available at <https://doi.org/10.1038/s41598-026-48651-8>.

**Correspondence** and requests for materials should be addressed to S.R.K.S.

**Reprints and permissions information** is available at [www.nature.com/reprints](http://www.nature.com/reprints).

**Publisher’s note** Springer Nature remains neutral with regard to jurisdictional claims in published maps and institutional affiliations.

**Open Access** This article is licensed under a Creative Commons Attribution-NonCommercial-NoDerivatives 4.0 International License, which permits any non-commercial use, sharing, distribution and reproduction in any medium or format, as long as you give appropriate credit to the original author(s) and the source, provide a link to the Creative Commons licence, and indicate if you modified the licensed material. You do not have permission under this licence to share adapted material derived from this article or parts of it. The images or other third party material in this article are included in the article’s Creative Commons licence, unless indicated otherwise in a credit line to the material. If material is not included in the article’s Creative Commons licence and your intended use is not permitted by statutory regulation or exceeds the permitted use, you will need to obtain permission directly from the copyright holder. To view a copy of this licence, visit <http://creativecommons.org/licenses/by-nc-nd/4.0/>.

© The Author(s) 2026